

Biodegradable single-polymer composites from polyvinyl alcohol

Andrea Dorigato · Alessandro Pegoretti

Received: 20 September 2011 / Revised: 16 November 2011 / Accepted: 17 November 2011 / Published online: 4 December 2011
© Springer-Verlag 2011

Abstract The microstructure and thermomechanical behaviour of a novel fully biodegradable polyvinyl alcohol (PVOH)-based single-polymer composite (SPC) is presented. Three kinds of PVOH stapled fibres, having different melting temperatures and tensile mechanical properties, were considered as a reinforcement, whilst plasticized PVOH granules were selected as a continuous matrix. Calorimetric tests on the constituents showed significantly different melting temperatures between the matrix and the fibres, thus evidencing adequate processing windows for the preparation of SPCs. On the other hand, scanning electron microscopy on the cryofractured surfaces of melt-mixed and compression-moulded SPCs experimentally proved that the morphological integrity of the reinforcement was maintained only when high melting temperature fibres were utilized. Quasi-static mechanical tensile tests highlighted the capability of the selected PVOH fibres to remarkably increase the elastic modulus, the stress at yield and the Vicat softening temperature of the PVOH matrix. Moreover, dynamic storage modulus and glass transition temperature of SPC increased with respect to the neat PVOH over the whole range of considered temperatures, whilst short-term creep stability was strongly improved, proportionally to the fibre content. The application of a time–temperature superposition principle to creep data confirmed the effectiveness of these fibres in increasing the long-term creep stability of the resulting materials.

Keywords Polyvinyl alcohol · Fibres · Single-polymer composites · Mechanical properties · Creep

Introduction

The interest of both scientific and industrial communities towards the use of polymer matrix composites (PMCs) in the replacement of more traditional structural materials, such as metals and ceramics, is continuously increasing [1]. In fact, PMCs offer several advantages over conventional materials, such as outstanding specific mechanical properties, ease of processing and good chemical resistance. High-strength fibres, such as glass, carbon, and aramid, have become the reinforcing materials of election because of their excellent mechanical properties and thermal stability. However, several environmental concerns have been recently arisen on their use as reinforcement for conventional plastics. In fact, current environmental legislation encourages manufacturers to carefully evaluate the environmental impact of their products at all stages of their life cycle, including recycling and final disposal [2]. On the other hand, it is well known that life cycle assessment of traditional composite materials does not yield favourable results in terms of the recyclability and energy requirements of the end-of-life processes [3]. Therefore, increasing attention is devoted to the use of natural fibres as alternatives to inorganic reinforcements. Natural fillers such as wood flour, starch and natural cellulose fibres are abundant, relatively cheap and fully biodegradable [4]. In most cases, they can be compounded with polymers to produce reinforced materials, retaining the more desirable properties of conventional plastics [5–7]. Even if these fillers derive from renewable resources and can be incinerated, natural fibre-based composites are generally not mechanically recyclable because

A. Dorigato (✉) · A. Pegoretti
Department of Materials Engineering and Industrial Technologies
and INSTM Research Unit, University of Trento,
via Mesiano 77,
38123 Trento, Italy
e-mail: andrea.dorigato@ing.unitn.it

the limited thermal stability of natural fillers may lead to severe thermal degradation during subsequent recycling or reprocessing steps [8].

A possible contribution to improve the recyclability of composites can be represented by the development of single-polymer composites (SPCs), an emerging class of materials characterized by several economic and ecological advantages over traditional composites [9]. They are also known as one-polymer composites, homocomposites, all polymer composites, self-reinforced or homogeneous composites [2, 10]. The peculiar characteristic of SPCs is that both the reinforcing and the continuous phases are polymers with the same chemical composition. The formation of a composite structure is possible for polymeric systems in which there is a proper difference between the melting point of the matrix and of highly oriented fibres (i.e. a processing window). The main advantage of SPCs is that, unlike traditional heterogeneous composites, they can be entirely melted down at the end of the product life, their recyclability being highly enhanced [11]. Another key factor is related to the fact that interfacial bonding can be considerably improved when the matrix and the reinforcement are made of the same polymer [12, 13]. The first example of these kinds of materials was reported in 1975 by Capiati and Porter [14] who introduced the concept of single-polymer composites by successfully preparing all-polyethylene composites. In the following years, several efforts were devoted by materials scientists and engineers to explore new materials combinations, to extend the processing window and to develop new processing techniques to be scaled up at an industrial level. Nowadays, the preparation of polyethylene [15–17], polypropylene [8, 11, 18, 19], poly(ethylene terephthalate) [20, 21], poly(methyl methacrylate) [22, 23], poly(ethylene naphthalate) [24] and liquid crystalline copolyesters [25] single-polymer composites has been extensively studied. Interestingly, less attention was devoted to biodegradable single-polymer composite systems. To the best of our knowledge, the only example of biodegradable SPCs is the preparation of a poly(lactic acid) SPC consisting of amorphous sheets as matrix and highly crystalline fibres, yarns and fabrics reported by Li and Yao [10]. In that case, significant improvements of the tensile strength and of the Young's modulus with respect to the neat matrix have been reported. Quite surprisingly, no papers dealing with the preparation of polyvinyl alcohol (PVOH)-based single-polymer composites can be found in the open scientific literature.

Poly(vinyl alcohol) is the only known carbon–carbon backbone polymer that is biodegradable under both aerobic and anaerobic conditions [26]. It has recently gained increasing attention both as a water-soluble biodegradable polymer and as a biodegradable segment in the polymer chain to be applied in a wide range of applications [27]. The hydroxyl groups present in its main backbone are

responsible for the strong intra- and intermolecular hydrogen bonds, endowing PVOH with many good properties, such as high tensile strength, excellent adhesive properties, abrasion resistance, chemical resistance and gas barrier properties [28]. Furthermore, PVOH is one of the few polymers which can be prepared via a non-petroleum route, i.e. by using natural gas as raw materials. For these reasons, PVOH is widely applied in many industrial applications, such as films, fibres, adhesives, textile sizing, emulsifiers, paper coating, etc. PVOH is produced on an industrial scale by hydrolysis (methanolysis) of poly(vinyl acetate) through a one-pot reaction. In this way, various PVOH grades can be obtained depending upon the degree of hydrolysis [29]. Even if plastic items based on polyvinyl alcohol are mainly obtained using casting techniques, increasing interest in the production of PVOH films stimulated the development of new melt processing technologies. The main difficulty to overcome during the thermal extrusion processing is the close proximity of its melting point and decomposition temperature. Consequently, the melt processing of PVOH requires its plasticization with relatively large amounts of water and organic plasticizers before extrusion. Several plasticizers, such as glycerol, ethylene glycol, amine alcohols and polyvalent hydroxyl compounds, can be utilized in the industrial field in order to enhance PVOH thermal stability [30].

Particular attention has been recently devoted to the development of PVOH fibres. Commercial production of PVOH fibres started in Japan after the Second World War, and nowadays, it is carried out by wet spinning or dry spinning, starting from aqueous PVOH solutions. In these processes, PVOH chips are dissolved in hot water and the solution is extruded through a spinneret. The extrudates are then coagulated to form continuous filaments and heat-treated to gain adequate mechanical properties. The water resistance of the fibres can then be improved by a heat treatment followed by acetalization. PVOH fibres present a high affinity for water due to the hydroxyl groups present in PVOH, excellent mechanical properties because of the high crystallinity, and elevated chemical resistance. PVOH fibres are mainly applied as concrete reinforcement. Like steel, PVOH fibres possess high tensile strength and a greater modulus of elasticity than regular concrete, but unlike steel, PVOH fibres develop a chemical bond with the cement during hydration and curing, increasing therefore their pull-out resistance. PVOH fibres are also effective in controlling the shrinkage and the fatigue cracking of traditional concretes [31]. In addition, PVOH fibres can be applied in several industrial applications, including rubber hosing reinforcement, geogrid reinforcement, paper and non-woven applications.

Starting from these considerations, the objective of the present paper was to develop biodegradable PVOH-based

single polymer composites with improved mechanical properties and dimensional stability.

Experimental part

Materials

PVOH chips (Mowiflex TC, density=1.27 gcm⁻³, MFI at 2.16 kg and 190 °C=39 g (10 min)⁻¹), supplied by Kuraray Specialties Europe GmbH (Frankfurt, Germany), were utilized as the matrix. Three different kinds of Kuralon® fibres (WN2, WN4, WN8), supplied by Kuraray Co. Ltd. (Tokyo, Japan), were considered as the reinforcement. These fibres were provided in the form of staples, having a mean length of 38 mm and a titre of 1.7 dTex. According to the producer's datasheet, they differ in the water dissolution temperatures (20, 40 and 80 °C for WN2, WN4 and WN8, respectively). Their density values, measured through an Accupyc 1330 helium pycnometer, are similar (i.e. 1.37, 1.36 and 1.39 gcm⁻³ for WN2, WN4 and WN8, respectively).

Preparation of the samples

Because of the marked tendency of PVOH fibres to adsorb moisture, they were dried at 60 °C for 6 h before to be compounded with PVOH chips in a Thermo Haake internal mixer operating at 180 °C for 6 min. These processing parameters were selected in order to obtain a good dispersion of the fibres avoiding thermal degradation of the matrix. Square sheets of composite samples with a mean thickness of about 1 mm were prepared by compression moulding the resulting materials at 180 °C for 5 min in a Carver laboratory press under a pressure of about 1 MPa. In order to prevent moisture absorption, samples were sealed in vacuum plastic bags under vacuum. Samples were designated indicating the matrix, the kind of fibre and its relative weight amount. For instance, PVOH-WN2-20 indicates a composite sample filled with 20 wt.% of WN2 fibres.

Characterization of the constituents

Thermal properties of the constituents (neat matrix and stapled fibres) were evaluated through differential scanning calorimetry (DSC) tests using a Mettler DSC 30 apparatus. Samples were first heated from 0 to 280 °C at 10 °C min⁻¹, cooled down to 0 °C at the same rate and finally reheated up to 280 °C. Samples were tested under a constant nitrogen flow of 150 ml min⁻¹. In this way, it was possible to determine the melting (T_m) and the crystallization (T_c) temperatures of the constituents. The relative crystallinity degree (χ) was computed dividing the specific melting

enthalpy of the polymer (ΔH_m) by that of a fully crystalline PVOH (ΔH_0), taken as 161 Jg⁻¹ [32], i.e.

$$\chi = \frac{\Delta H_m}{\Delta H_0} \quad (1)$$

Quasi-static tensile tests on the neat matrix and on dried fibres were performed at room temperature using an Instron 4502 tensile testing machine. Tensile properties of the neat matrix were determined by testing ISO 527 1BA dumbbell specimens, 5 mm wide and 1 mm thick, with a gage length of 30 mm punch-cut from the compression-moulded sheets. For the evaluation of the elastic modulus, a crosshead speed of 0.25 mm min⁻¹ was imposed to the samples and the strain was recorded through an Instron® model 2620-601 resistance extensometer (gage length=12.5 mm). Tensile test at break were carried out at a crosshead speed of 50 mm min⁻¹ without using the extensometer. At least five specimens were tested for each sample.

Tensile properties of the fibres were determined using the same machine, equipped with a 10-N load cell. Single filaments were extracted from the fabrics and glued on paper mounting tabs. Before testing, each specimen was preliminarily observed with an Ortholux II POL-BK optical microscope at a magnification of 40× in order to determine the fibre diameter. A crosshead speed of 1 mm min⁻¹ and a gage length of 20 mm was utilized for all the samples. In this way, it was possible to measure the elastic modulus (E), taken as the secant modulus between the deformation levels of 0.1% and 0.5%, the stress (σ_b) and the strain (ϵ_b) at break values. The distribution of the tensile strength of the fibres was statistically analysed applying an iterative procedure proposed by Gurvich et al. [33] starting from the Weibull approach [34]. The cumulative distribution of the stress at break of fibres $F(\sigma_b, V)$ having a generic volume $V=k \cdot V_0$ can be modelled as:

$$F(\sigma_b, V) = 1 - \exp \left[- \frac{V}{V_0} \left(\frac{\sigma_b}{\sigma_0} \right)^m \right] \quad (2)$$

where V_0 is the reference volume whilst σ_0 and m are the scale and the shape parameters of the distribution function, respectively. If a reduced stress $s = \sigma_b \cdot k^{1/m}$ is considered, the cumulative distribution of s can be written as follows:

$$F(s) = 1 - \exp \left[- \left(\frac{s}{\sigma_0} \right)^m \right] \quad (3)$$

If stress at break data are numbered in an ascending order with an index i , a cumulative failure probability can be estimated as $P_i = (i - 0.5)/n$ and inserted in Eq. 3, which can be linearized as follows:

$$\ln \left[\ln \left(\frac{1}{1 - P_i} \right) \right] = m \ln(s) - m \cdot \ln(\sigma_0) \quad (4)$$

σ_0 and m values can be evaluated defining an initial tentative m value and applying an iterative least square fitting procedure until the error falls below a desired value [33].

Characterization of the composites

Scanning electron microscopy (SEM) images of the fracture surfaces of the composites were obtained through a field emission Zeiss Supra 40 microscope at different magnifications. Samples were cryofractured in liquid nitrogen and metalized before observations. Differential scanning calorimetry tests were performed by using the DSC machine described in “Characterization of the constituents”.

Tensile mechanical tests were performed with the same equipment and with the same conditions utilized for the mechanical tests on the neat matrix and described in “Characterization of the constituents”. The determination of the Vicat softening temperature was performed with a HDT-Vicat mod. MP/3 (ATS FAAR) apparatus according to the ASTM D1525-07 standard. Rectangular specimens, 3.2 mm thick, 10 mm long and 5 mm wide, were utilized. The parameters used were: load, 10 N; initial temperature, 30 °C; heating rate, 50 °C h⁻¹. Three specimens were tested for each sample. Dynamic–mechanical properties (storage modulus, loss tangent) were determined as a function of temperature through a DMA Q800 (TA Instruments) apparatus in tensile configuration under the following conditions: clamp distance, 12 mm; frequency, 1 Hz; preload, 0.01 N; and strain amplitude, 64 μm. Specimens were heated at a rate of 3 °C min⁻¹ in the temperature range from 0 to 170 °C.

Creep tests at a constant stress of 3 MPa were performed using an Instron 4502 testing machine at various temperatures in the range from 30 to 90 °C. Rectangular specimens, 40 mm long, 5 mm wide and 0.8 mm thick, were utilized. A tensile creep compliance, $D(t)$, was computed by dividing the time-dependent strain, $\varepsilon(t)$, by the applied stress (σ_0). The total duration of the tests was 3,600 s. A time–temperature superposition principle was adopted to analyse the creep data on the basis of the following equation [35]:

$$D(\log t + \log a_{T_0}, T) = D(\log t \cdot a_{T_0}, T) = D(\log t, T_0) \quad (5)$$

where a_{T_0} is the time shift factor necessary to superimpose an isothermal curve collected at a temperature T on that measured at a given temperature T_0 . Master curves at a reference temperature $T_0=30$ °C were hence obtained, describing the creep response over a wide timescale.

Results and discussion

Characterization of the constituents

The DSC thermograms of PVOH chips are reported in Fig. 1 together with those of WN2, WN4 and WN8 fibres, whilst some relevant results are summarized in Table 1. It can be noticed that PVOH granules are characterized by a melting temperature (176.5 °C) and a crystallinity content (about 16%) much lower than those of PVOH fibres. This means that chain alignment produced during the spinning process and the subsequent drawing operations promoted some crystallization of the fibres, with the formation of a more regular and stable crystalline phase. It is also interesting to note that both T_m and χ values of the PVOH fibres remarkably increase moving from WN2 to WN4 and WN8 type of fibres. Considering the DSC results from the second heating stage, it can be noticed that crystallization during cooling at 10 °C min⁻¹ under quiescent conditions induces some changes in the microstructure of the materials under investigation. The observed changes for PVOH chips are relatively small, both T_m and χ values being only slightly increased. On the other hand, in the case of PVOH, a remarkable decrease of both melting point and crystallinity content can be observed in the second DSC heating stage. Among the investigated fibres, WN8 still manifest the highest T_m and χ values among the tested fibres even after the second heating stage. This means that the differences in the thermal properties of the tested fibres are not only due to the processing (stretching) conditions but also to possible differences in the molecular weight and/or hydrolysis degree of the parent polymers. In fact, it is widely reported in the literature that both the thermal and the mechanical properties of polyvinyl alcohol are strongly influenced by the

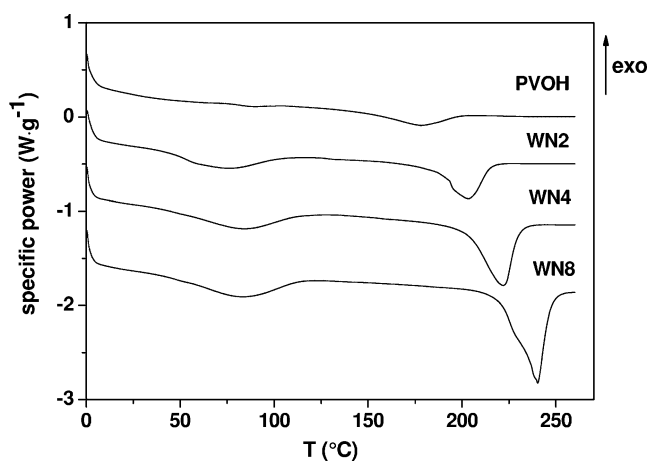


Fig. 1 First heating DSC thermograms of PVOH chips and WN2, WN4 and WN8 PVOH fibres

Table 1 Results of DSC tests on PVOH chips and on WN2, WN4 and WN8 PVOH fibres

Sample	First heating			Cooling			Second heating		
	T_{m1} (°C)	ΔH_{m1} (J g ⁻¹)	χ_1 (%)	T_c (°C)	ΔH_c (J g ⁻¹)	χ_c (%)	T_{m2} (°C)	ΔH_{m2} (J g ⁻¹)	χ_2 (%)
PVOH	176.5	25.2	15.7	127.0	–	–	180.0	19.1	11.9
WN2	202.4	50.5	31.3	149.3	37.1	23.0	198.2	36.8	23.4
WN4	220.3	79.1	49.1	172.7	52.4	32.5	211.3	50.7	31.5
WN8	238.6	99.4	61.7	188.7	65.7	40.8	222.3	67.9	42.2

T_{m1} melting temperature (first heating), ΔH_{m1} specific melting enthalpy (first heating), χ_1 relative crystallinity (first heating), T_c crystallization temperature, ΔH_c specific crystallization enthalpy, χ_c relative crystallinity (cooling), T_{m2} melting temperature (second heating), ΔH_{m2} specific melting enthalpy (second heating), χ_2 relative crystallinity (second heating)

aforementioned parameters [36]. However, DSC tests put in evidence the existence of a thermal processing window for the preparation of PVOH-based single polymer composites by using the three PVOH fibres.

The tensile mechanical properties of the neat PVOH sheets and of the three kinds of PVOH fibres are collected in Table 2. Neat PVOH matrix presents a ductile behaviour, with a relatively low elastic modulus and elevated deformation at break. As expected, the PVOH fibres present much higher elastic modulus and stress at break, with values increasing from WN2 to WN8, with a parallel reduction of the deformation at break. In order to provide a more detailed description of the fracture resistance of the PVOH fibres, a statistical approach based on the Weibull cumulative distribution is considered. In Fig. 2, the cumulative distributions of the stress at break data of PVOH fibres, with the fitting lines according to the expression reported in Eq. 4, are reported. The appropriateness of the Weibull distribution in fitting the strength data is supported by a coefficient of determination (R^2) higher than 0.87 for all the tested fibres (see Table 2). It is interesting to note that the scale parameter (σ_0) referred to a gage length of 20 mm increases with the water dissolution temperature (i.e. in the order WN2 < WN4 < WN8). It is worthwhile to observe that also the shape parameter (m) increases in the same order from WN2 to WN8. Considering that this parameter is directly related to the width of the statistical distribution of strength data [34], the higher m value detected for WN8 specimens accounts for a better mechanical reliability of these fibres.

Table 2 Tensile mechanical properties of neat PVOH compression-moulded sheets and of WN2, WN4 and WN8 PVOH fibres

Sample	E (MPa)	σ_y (MPa)	σ_b (MPa)	ϵ_b (%)	σ_0 (MPa)	m	R^2
PVOH	315±20	33.6±2.4	43.6±6.4	280±80	–	–	–
WN2	9,600±1,100	–	425.9±95.7	19±2	581.1	4.8	0.865
WN4	12,500±2,500	–	673.0±119.8	14±3	809.2	6.5	0.948
WN8	22,400±1,500	–	883.6±112.4	9±1	1,048.9	7.7	0.972

Characterization of the composites

The results of DSC tests on the neat PVOH and relative composites with a fibre content of 20 wt.% are summarized in Table 3. The melting endothermal signals of two distinct phases can be clearly distinguished in the DSC scans of SPCs under investigation (not reported for brevity). It is interesting to note that both the melting temperature (T_{m2}) and the crystallinity degree (χ_2) of the compounded fibres are lower than the values reported in Table 2 for the unprocessed fibres. This is a clear indication that the selected processing conditions produced a partial melting of low crystallinity fractions of the fibres. This phenomenon could have been enhanced by a possible overheating produced by the high shear stresses generated during the melt compounding process. A reduction of the fibre crystallinity may negatively affect their reinforcing capability in the composites. However, this is only a hypothesis since a direct evaluation of the effect of the thermomechanical degradation induced by the melt compounding on the mechanical properties of the fibres is practically impossible.

In order to investigate the fibre morphology within the SPCs, microstructural analyses were carried out by electron microscopy. SEM images of the fracture surfaces of the neat PVOH matrix and of SPC samples at a fibre loading of 20 wt.% are reported in Fig. 3. As expected, the fracture surface of the neat PVOH matrix is relatively smooth. It is interesting to note how in PVOH-

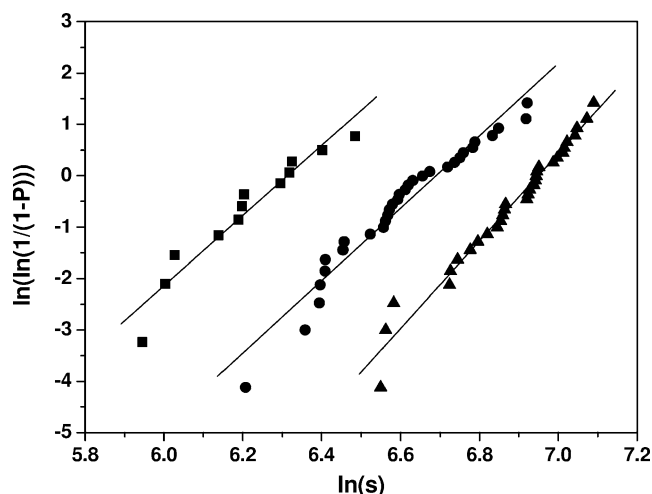


Fig. 2 Strength distribution of WN2 (square), WN4 (circle) and WN8 (triangle) fibres where the linear fitting lines follow the Weibull distribution (see Eq. 4)

WN2-20 and PVOH-WN4-20 samples the fibrous morphology is almost completely lost. This means that the selected processing conditions cannot prevent a partial melting of this type of fibres. A completely different situation can be found in WN8-filled composite. In this case, the fibrous morphology of the reinforcement is maintained and some cavities due to the debonding phenomena can be clearly detected. The length of the protruding fibres is lower than 20 μm , thus indicating that a relatively good level of fibre–matrix interfacial adhesion has been reached [37]. This positive result can be attributed to the fact that both matrix and fibres have the same chemical nature. From these preliminary results, it clearly emerges that WN8 fibres is the optimal choice for the preparation of full PVOH composites with fibrous morphology, possessing suitable thermal and dimensional stability.

Therefore, WN8 fibres were selected for the preparation of composites with fibre concentrations of 10, 20 and 30 wt. % whose SEM images of the fracture surfaces are reported in Fig. 4. From these micrographs, we can have an indica-

tion that dispersed fibres assume a random orientation in the composite, and no substantial differences can be noticed as the fibre fraction changes. In all cases, a fibrous morphology is preserved and some voids due to fibre–matrix interfacial debonding can be observed.

Representative stress–strain curves from quasi-static tensile tests on the neat PVOH matrix and the composites filled with various amounts of WN8 fibres are reported in Fig. 5a, b, whilst the most important parameters are collected in Table 4. In Fig. 5a, where the initial (small strain) region of the tensile curves is enlarged, it can be noticed that the addition of the fibres produces an interesting stiffening effect. In fact, as reported in Table 4, the tensile modulus increases by a factor of about 6 when 30 wt.% of WN8 fibres are added to the PVOH matrix.

In order to interpret these results, it could be useful to model elastic modulus data giving insight into whether the process has changed the properties and/or the aspect ratio of the fibres. Several models were developed in the last decades to model the elastic properties of short-fibre-reinforced composites [38–42], taking also into account the effect of fibre misalignment [43]. Considering that, as reported earlier, the selected manufacturing process is very likely to produce a random distribution of short fibres, we tried to model elastic modulus data by using the Halpin–Tsai model in which the dependency of elastic constants from the fibre length and the fibre modulus is accounted [44].

According to the Halpin–Tsai model, the moduli of short fibre composites with fibres perfectly aligned along the strain direction (E_L) or with fibres orientated transversally to strain direction (E_T) can be evaluated as [45]:

$$E_L = \frac{1 + 2(l/d)(\eta_L \varphi)}{1 - \eta_L \varphi} E_M \quad (6)$$

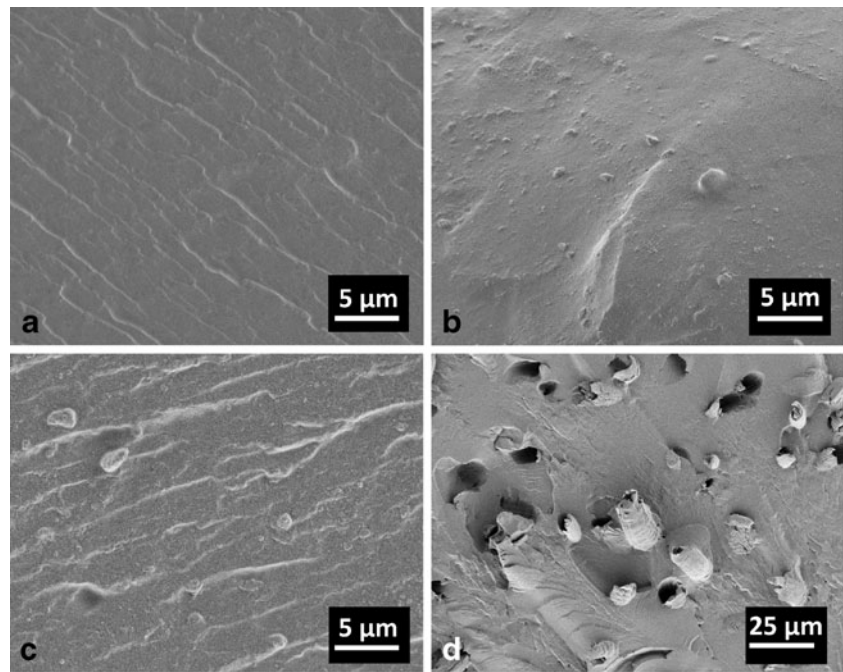
$$E_T = \frac{1 + 2\eta_T \varphi}{1 - \eta_T \varphi} E_M \quad (7)$$

Table 3 Results of DSC tests on neat PVOH and relative composites (fibre content=20 wt.%)

Sample	T_{m1} (°C)	T_{m2} (°C)	ΔT (°C)	ΔH_{m1} (J g ⁻¹)	χ_1 (%)	ΔH_{m2} (J g ⁻¹)	χ_2 (%)
PVOH	176.5	–	–	25.2	15.7	–	–
PVOH-WN2-20	176.2	194.5	18.4	11.7	7.3	16.9	10.5
PVOH-WN4-20	173.7	195.0	21.3	10.7	6.6	47.5	29.5
PVOH-WN8-20	173.2	221.2	47.9	17.3	5.3	65.5	21.0

T_{m1} melting temperature (first heating), ΔH_{m1} specific melting enthalpy (first heating), χ_1 relative crystallinity (first heating), T_{m2} melting temperature (second heating), ΔH_{m2} specific melting enthalpy (second heating), χ_2 relative crystallinity (second heating)

Fig. 3 SEM images of the fracture surfaces of neat PVOH and relative composites at a fibre content of 20 wt.%. PVOH (a), PVOH-WN2-20 (b), PVOH-WN4-20 (c), PVOH-WN8-20 (d)



and

$$\eta_L = \frac{(E_F/E_M) - 1}{(E_F/E_M) + 2(l/d)} \quad (8a)$$

$$\eta_T = \frac{(E_F/E_M) - 1}{(E_F/E_M) + 2} \quad (8b)$$

where l/d is the aspect ratio of the fibres, Φ is the volume fraction of the fibres, and E_F and E_M are the fibre and matrix moduli, respectively. Finally, the tensile modulus of randomly oriented fibre composites (E) can be expressed as:

$$E = \frac{3}{8}E_L + \frac{5}{8}E_T \quad (9)$$

Considering that the adopted processing method (melt mixing and compression moulding) could produce a significant breakage of the fibre and/or a reduction of their mechanical properties, it could be interesting to model the effect of both fibre length and modulus. Figure 6a compares the relative elastic modulus values of the prepared samples with theoretical predictions obtained at various fibre lengths. Knowing the density of the matrix and of the fibres, the relative weight fractions were translated into the corresponding volume concentration, whilst WN8 fibre diameter ($11.3 \mu\text{m}$) was determined through optical microscope observations. It is evident that theoretical predictions with the original fibre length (38 mm) largely overestimate experimental results, and a good fitting could be obtained only if a very limited fibre length is considered (0.23 mm). On the other hand, Fig. 6b shows that, if a fibre

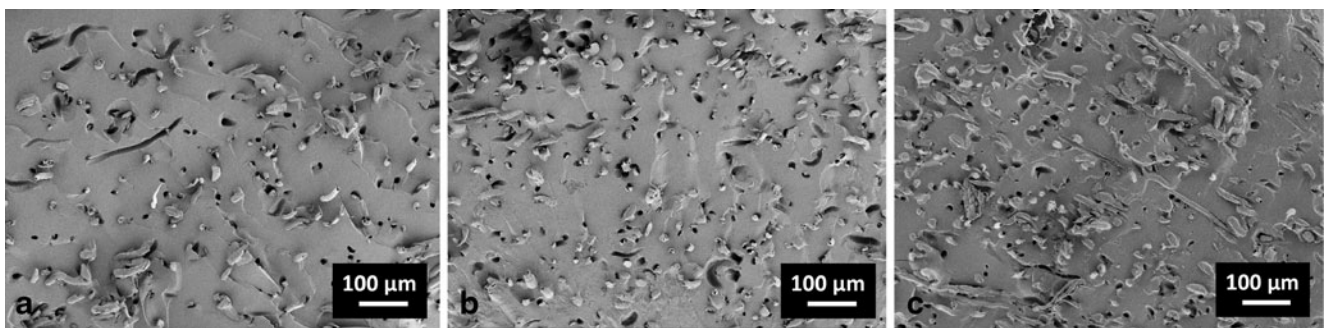


Fig. 4 SEM images of the fracture surface of composites filled with various amounts of WN8 fibres: PVOH-WN8-10 (a), PVOH-WN8-20 (b), PVOH-WN8-30 (c)

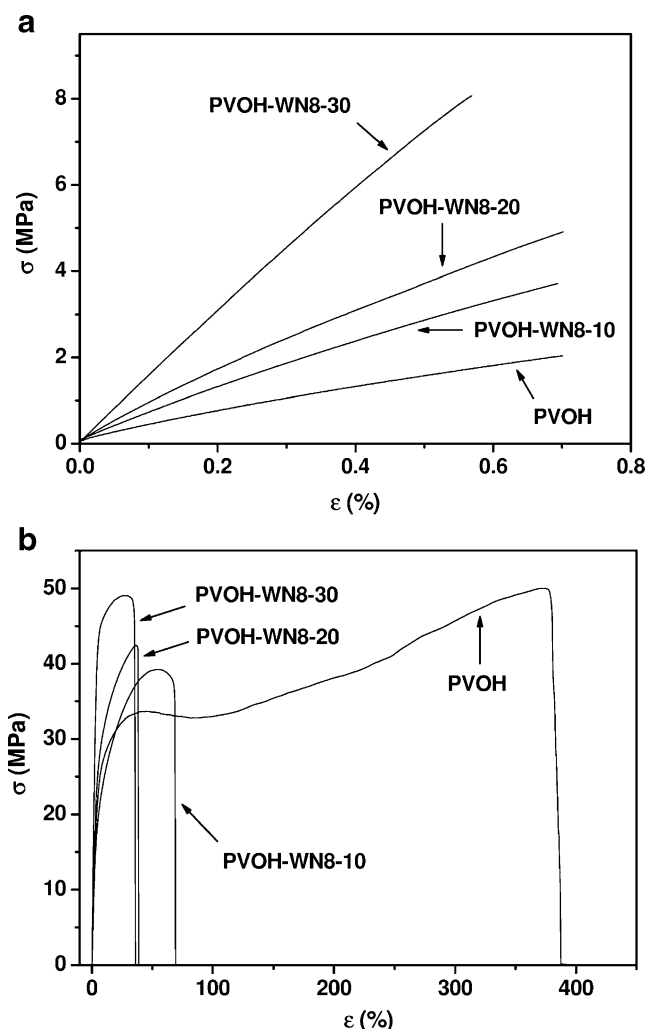


Fig. 5 Representative stress–strain curves under quasi-static tensile tests on the neat PVOH and composites filled with various amounts of WN8 fibres. Low strain region (a) and tensile tests up to failure (b)

length of 38 mm is assumed, a satisfactory fit with the experimental results could be obtained only considering a significant reduction of the original fibre stiffness. In the absence of a direct in situ measurement of fibre length and/or modulus, we can only suppose that the observed reinforcing capability of the fibres is due to a combination of these two factors.

Table 4 Tensile mechanical properties and Vicat softening temperature of neat PVOH and WN8-filled composites

Sample	E (MPa)	σ_y (MPa)	σ_b (MPa)	ε_b (%)	Vicat softening temperature (°C)
PVOH	315±20	33.6±2.4	43.6±6.4	280±80	126.4±1.5
PVOH-WN8-10	599±74	36.9±2.8	32.2±4.3	64±19	156.9±3.3
PVOH-WN8-20	831±89	43.1±6.5	42.1±6.0	42±20	161.1±1.0
PVOH-WN8-30	1,803±218	51.2±3.4	48.5±4.0	36±18	172.3±2.2

Figure 5b evidences that the neat matrix shows a ductile behaviour, with a relatively low yield point and elevated strain at break. Stress at yield values (σ_y) are enhanced by fibre addition passing from the value of 33.6 MPa of the neat matrix to 51.2 MPa for the PVOH-WN8-30 sample. On the other hand, strain at break (ε_b) is heavily reduced upon fibre addition (Fig. 5b and Table 4), passing from 280% for the neat matrix to 36% for the 30 wt. % filled composite. The significant lowering of ε_b is also inducing a relevant decrease of the tensile energy to break of the material.

In order to evaluate the dimensional stability of the prepared composite, Vicat softening temperature (VST) measurements were carried out. In fact, the Vicat softening temperature, defined as the temperature at which a flat-ended probe of 1-mm² circular cross-section penetrates the specimen to a depth of 1 mm under a specific load using a selected temperature ramp, is generally evaluated to assess the service temperature of polymeric materials [46]. As reported in Table 4, the Vicat grade noticeably increases with the fibre fraction. For instance, PVOH-WN8-10 composite shows a VST about 30 °C higher than that of the neat PVOH, whilst the Vicat grade of PVOH-WN8-30 sample reaches a value of 172.3 °C, i.e. very close to the melting temperature of the PVOH matrix.

The contribution of PVOH fibres on the viscoelastic properties of the SPC composites has been investigated through dynamic mechanical thermal analysis and creep tests. The temperature dependence of storage modulus (E') and loss tangent ($\tan\delta$) values of neat PVOH and composites reinforced with various amounts of WN8 fibres are reported in Fig. 7a, b, respectively. As commonly happens for semi-crystalline polymers, a drastic drop of the storage modulus is observed in correspondence of the glass transition temperature due to the material transition from a glassy to a rubbery state. The presence of WN8 fibres increases the storage modulus over the entire temperature range. Furthermore, the glass transition temperature, evaluated in correspondence of the $\tan\delta$ peak, also increases with the fibre content. Concurrently, the immobilizing effect provided by the fibres induces a strong decrease of the $\tan\delta$ peak. Isothermal creep compliance curves of neat PVOH and composites filled with WN8 fibres are reported in Fig. 8. Also in

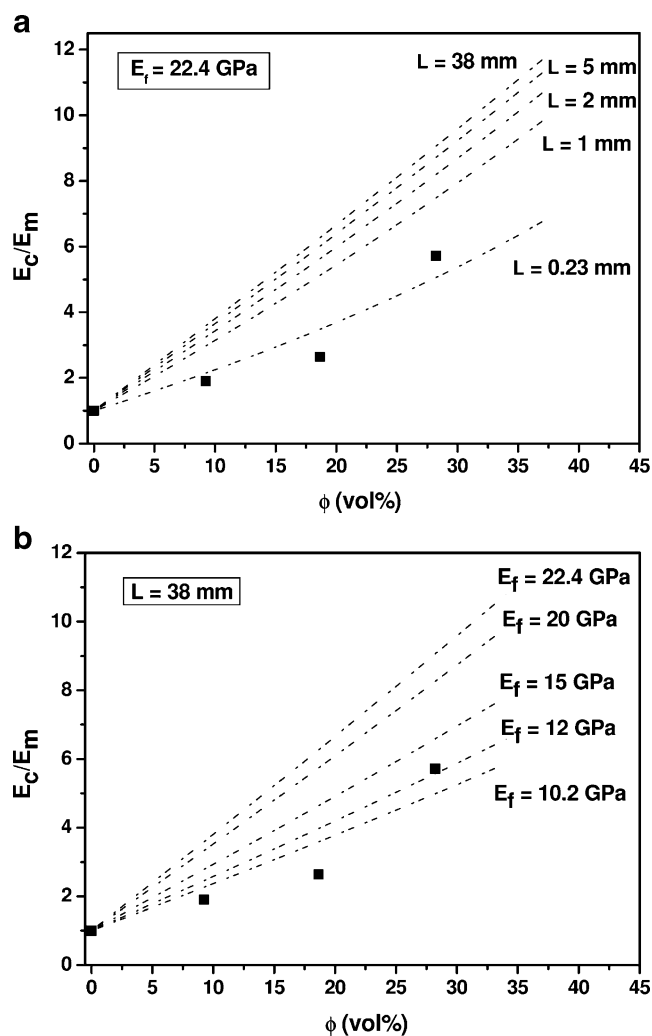


Fig. 6 Relative elastic modulus values of the neat PVOH and composites filled with various amounts of WN8 fibres, with the fitting lines according to theoretical predictions (Eqs. 6–9, dashed lines). **a** Effect of the fibre length. **b** Effect of the fibre modulus

this case, the stabilizing effect provided by PVOH fibres is manifested in a progressive reduction of the creep compliance values. After a loading time of 3,600 s, the neat matrix shows a creep compliance of about 14 GPa^{-1} , whilst the PVOH-WN8-30 composite reaches a value of only 3 GPa^{-1} . These results could be particularly important for those applications for which a good dimensional stability under constant loads is required at ambient temperature. In order to evaluate the effect of the temperature on the creep stability of these materials, creep tests at various temperatures were carried out under a constant stress of 3 MPa. Creep compliance curves of neat PVOH and PVOH-WN8-30 composites at various temperatures are reported in Fig. 9a, b, respectively. It is interesting to note that the stabilizing effect provided by the

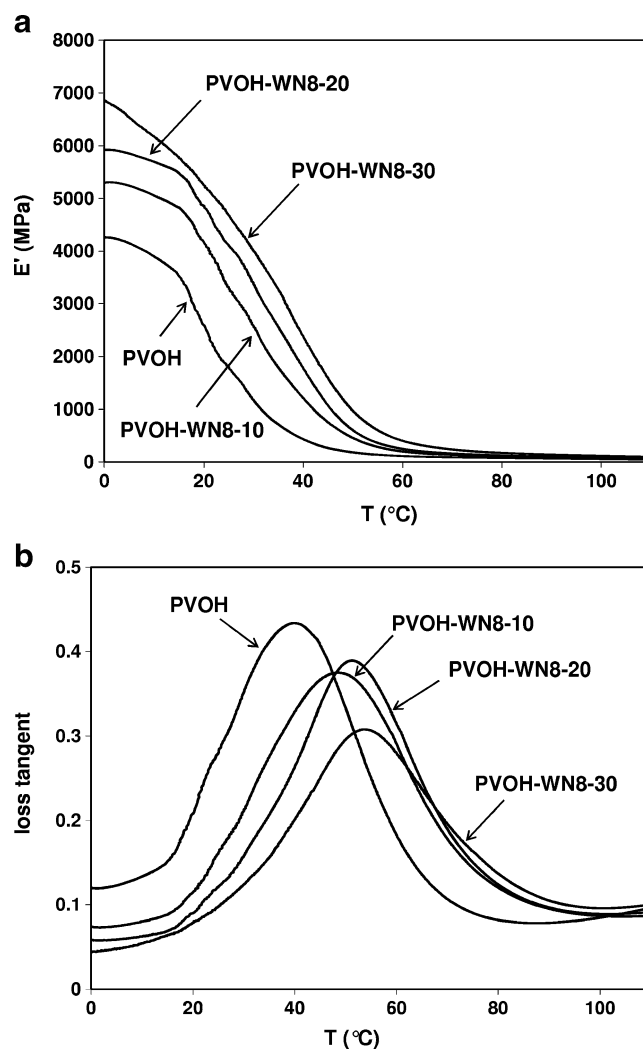


Fig. 7 DMTA tests on neat PVOH and composites filled with various amounts of WN8 fibres. **a** Storage modulus (E'). **b** Loss tangent ($\tan\delta$)

PVOH fibres is maintained also at elevated temperatures. In fact, if creep compliance values after 3,600 s and at a temperature of 90 °C are compared, the PVOH-WN8-30 composite shows a value five times lower than that registered for the neat PVOH matrix. In order to describe the viscoelastic behaviour over a wide timescale, creep compliance master curves at a reference temperature (T_0) of 30 °C and a reference stress (σ_0) of 3 MPa were generated on the basis of a time–temperature superposition principle (see Eq. 5). In Fig. 9c, the obtained master curves are reported. It is evident that a good superposition can be obtained for both neat PVOH and for filled samples, and the dramatic reduction of the creep compliance with the fibre content is confirmed over an extended time interval. In fact, whilst for the neat PVOH matrix a creep

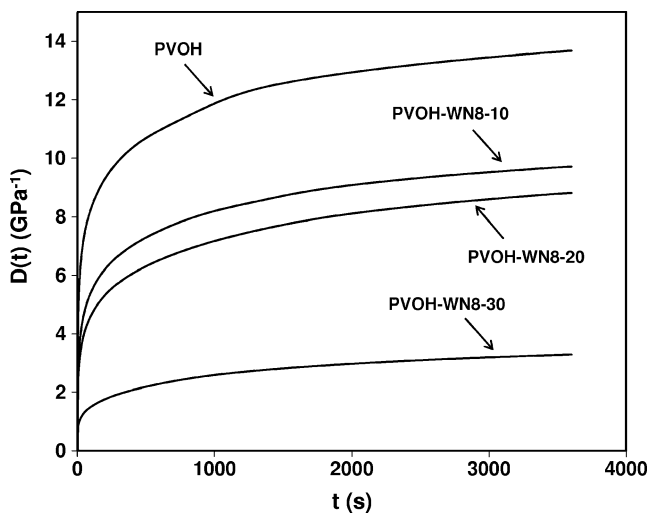


Fig. 8 Creep compliance curves at a temperature of 30 °C and applied stress $\sigma_0=3$ MPa for neat PVOH and composites filled with of WN8 fibres

compliance of 20 GPa^{-1} can be estimated after a loading time of 1 day, for the PVOH-WN8-30 sample, a time period of about 12 years is needed to reach the same creep compliance.

Conclusions

For the first time, fully biodegradable polyvinyl alcohol (PVOH)-based single polymer composites (SPCs) were prepared through a melt compounding process and thermomechanically characterized. Three kinds of stapled PVOH fibres, differing in their melting temperatures and tensile properties, were considered. Even if DSC tests on the constituents highlighted the theoretical possibility to prepare single-polymer composites with an adequate processing window, SEM images on the cryo-fractured surfaces evidenced how the reinforcement morphology was maintained only when high melting temperature fibres were utilized. The introduction of PVOH fibres effectively increased the stiffness, the yield properties and the Vicat softening temperature of the neat PVOH matrix proportionally to the fibre content. On the other hand, a progressive reduction of the elongation at break was encountered for the filled samples. The stabilizing effect due to fibre introduction was confirmed by marked improvements of the viscoelastic properties of the composites. The storage modulus and glass transition temperature of SPC increased with respect to the neat matrix, whilst creep compliance values were strongly decreased at all the tested temperatures.

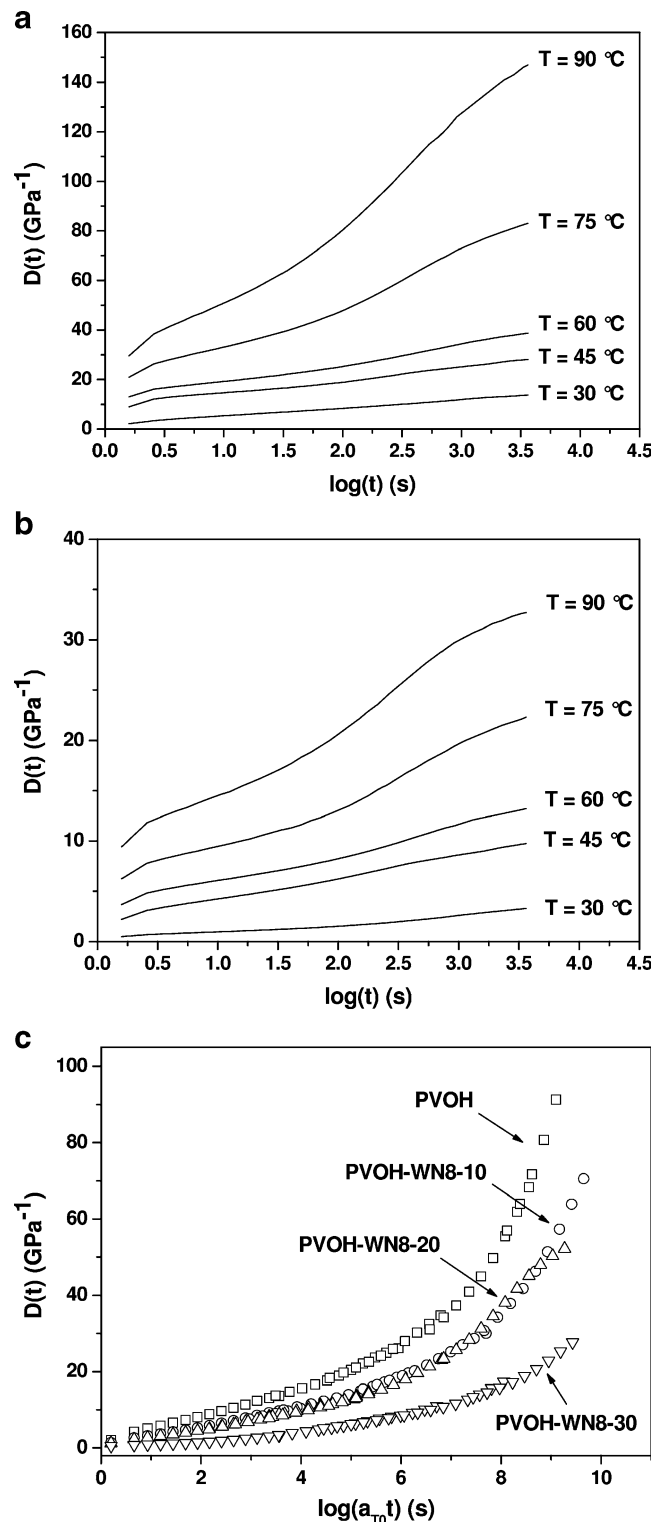


Fig. 9 Effect of temperature on the creep compliance curves under an applied stress $\sigma_0=3$ MPa for the neat PVOH (a) and PVOH-WN8-30 composite (b). c Creep compliance master curves at a reference temperature $T_0=30$ °C obtained on the basis of a time–temperature superposition principle

Acknowledgements Mr. Roberto Svarca is gratefully acknowledged for his support to the experimental work. We also thank Mr. Massimo Bricchi (Sales Manager Marketing Italy PVA/PVB of Kuraray Europe) of Seppic Italia Srl for his help in selecting the investigated materials.

References

- Gay D, Hoa SV, Tsai SW (2003) Composite materials: design and applications. CRC, Boca Raton
- Pegoretti A (2007) Trends in composite materials: the challenge of single-polymer composites. *eXPRESS Polym Lett* 1(11):710. doi:10.3144/expresspolymlett.2007.97
- Henshaw JM, Han W, Owens AD (1996) An overview of recycling issues for composite materials. *J Thermoplast Compos Mater* 9(1):4–20. doi:10.1177/089270579600900
- Wu C-S (2009) Renewable resource-based composites of recycled natural fibers and maleated polylactide bioplastic: characterization and biodegradability. *Polym Degrad Stab* 94(7):1076–1084. doi:10.1016/j.polyimdegradstab.2009.04.002
- García M, Garmendia I, García J (2008) Influence of natural fiber type in eco-composites. *J Appl Polym Sci* 107(5):2994–3004. doi:10.1002/app.27519
- Iwatake A, Nogi M, Yano H (2008) Cellulose nanofiber-reinforced polylactic acid. *Compos Sci Technol* 68(9):2103–2106. doi:10.1016/j.compscitech.2008.03.006
- Kunanopparat T, Menut P, Morel M, Guilbert S (2008) Reinforcement of plasticized wheat gluten with natural fibers: from mechanical improvement to deplasticizing effect. *Compos Part A Appl Sci Manuf* 39(5):777–785. doi:10.1016/j.compositesa.2008.02.001
- Houshyar S, Shanks RA (2003) Morphology, thermal and mechanical properties of poly(propylene) fibre–matrix composites. *Macromol Mater Eng* 288(8):599–606. doi:10.1002/mame.200300023
- Kmetty A, Barany T, Karger-Kocsis J (2010) Self-reinforced polymeric materials: a review. *Prog Polym Sci* 35(10):1288–1310. doi:10.1016/j.progpolymsci.2010.07.002
- Li R, Yao D (2008) Preparation of single poly(lactic acid) composites. *J Appl Polym Sci* 107(5):2909–2916. doi:10.1002/app.27406
- Alcock B, Cabrera N, Barkoula N, Spoelstra A, Loos J, Peijs T (2007) The mechanical properties of woven tape all-polypropylene composites. *Compos Part A Appl Sci Manuf* 38(1):147–161. doi:10.1016/j.compositesa.2006.01.003
- Deng M, Shalaby SW (1997) Properties of self-reinforced ultrahigh-molecular-weight polyethylene composites. *Biomaterials* 18:645–655
- Mosleh M, Suh NP, Arinez J (1998) Manufacture and properties of a polyethylene homocomposite. *Compos Part A* 29A:611–617
- Capiati NJ, Porter RS (1975) The concept of one polymer composites modeled with high density polyethylene. *J Mater Sci* 10:1671–1677
- Lacroix FV, Lu HQ, Schulte K (1999) Wet powder impregnation for polyethylene composites: preparation and mechanical properties. *Compos Part A* 30:369–373
- Ogawa T, Mukai H, Osawa S (1998) Mechanical properties of ultrahigh-molecular-weight polyethylene fiber-reinforced PE composites. *J Appl Polym Sci* 68:1431–1439
- Pegoretti A, Ashkar M, Migliaresi C, Marom G (2000) Relaxation processes in polyethylene fibre-reinforced polyethylene composites. *Compos Sci Technol* 60:1181–1189
- Houshyar S, Shanks RA (2006) Mechanical and thermal properties of flexible poly(propylene) composites. *Macromol Mater Eng* 291(1):59–67. doi:10.1002/mame.200500306
- Loos J, Schimanski T, Hofman J, Peijs T, Lemstra PJ (2001) Morphological investigations of polypropylene single-fibre reinforced polypropylene model composites. *Polymer* 42:3827–3834
- Barkoula N-M, Peijs T, Schimanski T, Loos J (2005) Processing of single polymer composites using the concept of constrained fibers. *Polym Compos* 26(1):114–120. doi:10.1002/pc.20082
- Yao D, Li R, Nagarajan P (2006) Single-polymer composites based on slowly crystallizing polymers. *Polym Eng Sci* 46(9):1223–1230. doi:10.1002/pen.20583
- Gilbert JL, Ney DS, Lautenschlager EP (1995) Self-reinforced composite poly(methyl methacrylate): static and fatigue properties. *Biomaterials* 16:1043–1055
- Wright-Charlesworth DD, Lautenschlager EP, Gilbert JL (2005) Hot compaction of poly(methyl methacrylate) composites based on fiber shrinkage results. *J Mater Sci Mater Med* 16:967–975
- Hine PJ, Astruc A, Ward IM (2004) Hot compaction of polyethylene naphthalate. *J Appl Polym Sci* 93(2):796–802. doi:10.1002/app.20517
- Pegoretti A, Zanolli A, Migliaresi C (2006) Preparation and tensile mechanical properties of unidirectional liquid crystalline single-polymer composites. *Compos Sci Technol* 66(13):1970–1979. doi:10.1016/j.compscitech.2006.01.012
- Matsumura S, Toshima K (1996) Biodegradation of poly(vinyl alcohol) and vinyl alcohol block as biodegradable segment. In: Ottenbrite RM, Huang SJ, Park K (eds) *Hydrogels and biodegradable polymers for bioapplications*, vol 627. ACS Symposium Series, pp 137–148
- Matsumura S, Tomizawa N, Toki A, Nishikawa K, Toshima K (1999) Novel poly(vinyl alcohol)-degrading enzyme and the degradation mechanism. *Macromolecules* 32:7753–7761
- Chen N, Li L, Wang Q (2007) New technology for thermal processing of poly(vinyl alcohol). *Plast Rubber Compos Process Appl* 36(7):283–290. doi:10.1179/174328907x237575
- Chiellini E, Corti A, D'Antone S, Solaro R (2003) Biodegradation of poly(vinyl alcohol) based materials. *Prog Polym Sci* 28(6):963–1014. doi:10.1016/s0079-6700(02)00149-1
- Petrushenko EF, Vakanyan PS, Pakhrenko VA (1988) Rheological properties of poly(vinyl alcohol)-based compositions. *Plasticheskie Massy* 11:23–24
- Shao Y, Shah SP (1997) Mechanical properties of PVA fiber reinforced cement composites fabricated by extrusion processing. *Mater J* 64(6):555–564
- Dickstein J, Bouchard R (1964) *Polyvinyl alcohol. Manufacture of plastics*. Reinhold, New York
- Gurvich M, Di Benedetto A, Pegoretti A (1997) Evaluation of the statistical parameters of a Weibull distribution. *J Mater Sci* 32:3711–3716
- Weibull W (1951) A statistical distribution function of wide applicability. *J Appl Mech* 18:293–297
- Riande E, Calleja RD, Prolongo MG, Masegosa RM, Salom C (2000) *Polymer viscoelasticity*. Marcel Dekker, New York
- Finch CA (1973) *Polyvinyl alcohol. Properties and applications*. Wiley, Bristol
- Pegoretti A, Accorsi ML, DiBenedetto AT (1996) Fracture toughness of the fiber–matrix interface in glass–epoxy composites. *J Mater Sci* 31(23):6145–6153
- Cox HL (1952) The elasticity and strength of paper and other fibrous materials. *Brit J Appl Phys* 3:72–79
- Ericson M, Berglund L (1993) Processing and mechanical properties of orientated preformed glass-mat-reinforced thermoplastics. *Compos Sci Technol* 49:121–130

40. Rosenthal J (1992) A model for determining fiber reinforcement efficiencies and fiber orientation in polymer composites. *Polym Compos* 13:462–466
41. Thomason JL, Vlugs MA, Schipper G, Krikor HGLT (1996) Influence of fibre length and concentration on the properties of glass fibre-reinforced polypropylene: Part 3. *Strength Strain Fail Comp Part A* 27A:1075–1084
42. Pan N (1993) Theoretical determination of the optimal fiber volume fraction and fiber–matrix property compatibility of short fiber composites. *Polym Compos* 14:85–93
43. Krenchel H (1964) *Fibre reinforcement*. Akademisk Forlag, Copenhagen
44. Halpin JC, Kardos JL (1976) The Halpin–Tsai equations: a review. *Polym Eng Sci* 16(5):361–364
45. Halpin JC, Pagano NJ (1969) The laminate approximation for randomly oriented fibre composites. *J Compos Mater* 3:720–724
46. Namhata SP, Santolini L, Locati G (1990) Rationalization of Vicat softening point measurements. *Polym Test* 9(2):75–89